

Modeling a Wearable Full-body Motion Capture System

Christopher Einsmann, Meghan Quirk, Ben Muzal, Bharath Venkatramani, Thomas Martin, and Mark Jones
Virginia Polytechnic Institute and State University

Blacksburg, Virginia 24060 (0111)

Email: {ceinsman, quirk, bmuzal, bharathv, tlmartin, mtj}@vt.edu

Abstract—This paper describes a feasibility study for a self-contained, wearable full-body motion capture system based on time-of-flight measurements that provide absolute distances between points on the body. Our motivation for the system is to allow an e-textile garment to sense its own shape using only body-worn sensors, thereby enabling it to dynamically adapt its sensing and processing elements to the user's current pose. Furthermore, a garment that can sense its own shape would enable an untethered and self-contained motion capture system. We explore the potential accuracy of the system via simulation driven by motion data from several users performing various activities, including effects such as the number and placement of sensors on the torso, shadowing of signal transmission by the body, and sensor directionality. We conclude that the system is feasible, albeit with an accuracy that is at least an order of magnitude less than state-of-the-art laboratory systems, and that its accuracy will depend heavily upon the transmission properties of the sensors.

I. INTRODUCTION

Through our previous work on electronic textiles, we have realized that there is a difficult set of related problems that must be addressed if e-textiles are to reach their full potential for wearable computing: an e-textile garment must be able to sense the shape of the garment, the location of sensors on the garment, and the user's motions [1]. These closely related capabilities are important for e-textiles for several reasons: They allow the e-textile to manage the physical locality of computation and sensing, thereby balancing computational load and power consumption across the hardware elements. The e-textile can provide necessary information to applications about the locations of sensors and their spacing, which can be used to dynamically select sensors that are in the best position. More broadly, having a garment that can sense its own shape will enable the development of self-contained untethered motion capture systems, new human computer interfaces, and more adaptable context-awareness devices.

This paper studies the feasibility of capturing the dynamic shape of a garment with only body-worn, time-of-flight sensors, i.e., without assistance from the nearby environment. We focus on time-of-flight sensors (e.g., ultrasonic pulses) because they provide absolute distances, in contrast to rate-of-change sensors such as accelerometers and gyroscopes. The difficulty with rate-of-change sensors is that their output must be integrated to find distance, and any noise in the sensor output quickly adds up to create a large error in the integrated value. Furthermore, even if noise were not an issue,

integration requires a boundary condition to find the value of the integration constant. For some motions, this boundary condition exists, e.g., when walking, the velocity of the heel is zero immediately following the heel strike, but for most motions there are no apparent boundary conditions. Thus rate-of-change sensors would be difficult to use for this application.

The method we employ for this preliminary investigation is simulation driven by motion capture data [2]. The benefit of simulation is that it permits quick exploration of the design space, particularly with respect to number and placement of sensors body size, and activity. While our initial motivation is sensing the shape of e-textile garments, the results we present are not limited to e-textile implementations; they are generalizable to other forms of implementation, e.g., body-worn nodes that communicate wirelessly.

The remainder of the paper is organized as follows. Section II presents related work in e-textiles and motion capture systems. Section III discusses design issues for a wearable e-textile motion capture system. Section IV describes how the system was modeled while Section V presents the simulation results. Section VI outlines our conclusions and future work.

II. BACKGROUND

The two areas of research that are most closely related to this paper are electronic textiles and motion capture systems.

A. E-Textiles

Electronic textiles are fabrics that have interconnections, electronics, sensors, and processors as an intrinsic part of the cloth. An overview of many of the research issues for e-textiles is available in [3]. Space does not permit a full overview of existing research and prototypes here, but there are many examples that we are aware of both in academia [4] [5] [6] [7] and in industry [8] [9].

We believe the efficient development of e-textile applications will require significant software services support, services for fault tolerance, physical configuration, and processor selection [1]. The physical configuration service will depend heavily upon the shape-sensing capability that we are exploring in this paper. Many applications of e-textiles will intrinsically need to know the spacing between sensors, for example, acoustic beamforming for locating the direction of a sound source [10]. Other applications will benefit by knowing the shape of the garment so that they can adapt to improve their

behavior, e.g. which sensing or processing element is farthest to the user's left? This information can only be provided by dynamically sensing the garment's shape.

B. Motion Capture Systems

Our initial motivation for sensing the garment's shape is to provide the physical configuration service. Perhaps more importantly, however, the shape-sensing capability also enables the garment to be used as a self-contained motion capture system, with applications in biomechanical research, physical therapy and rehabilitation, computer animated graphics, and virtual reality. Motion capture systems track the locations of the body as the user moves about. An e-textile device for capturing the motion of small portions of the body such as the hands has already been demonstrated [11], so the focus in this section is on systems for tracking the whole body or large portions of it. Systems for tracking the whole body measure the geometries of the movement patterns of the body, using either videographic, optoelectronic, or electromagnetic devices. These classes of systems involve attaching markers to the user's body, recording the positions of those markers and then post-processing the recorded data [12].

There are two major drawbacks to state-of-the-art systems that prevent them from being more widely used: First, they require an expensive laboratory apparatus that constrains the user to a limited area. Second, the set-up and post-processing times are typically quite lengthy. Having a cost-effective, self-contained motion capture system that does not constrain the user to be in a limited, laboratory setting or require lengthy set-up/post-processing would allow many applications that are used mainly for research to be more widely available.

Unlike the motion capture systems described in the above paragraphs, the capability we are exploring in this paper will not track the user's motions relative to an external frame of reference. Motions will only be sensed relative to the user. For example, the system we are proposing would not be able to tell the difference between walking down a hallway and walking on a treadmill, assuming that the user makes exactly the same motions in both situations. However, adding sensors to find the user's location and the direction he is facing (e.g., GPS or other location awareness system for location and a digital compass for direction) would allow our system to incorporate an external frame of reference.

People have experimented with acoustic motion tracking previously with a variety of parameters from on-body sensors to sensors placed in the environment. Some virtual reality motion tracking work includes Foxlin's head-worn hand tracking device [13] and his acoustic system with sensors embedded in the environment [14]. Each of these systems shows that acoustic tracking is viable, however, the final form is either cumbersome for the wearer or not self-contained, and confines the user to a limited area.

Research more closely related to our work is Vallidis's WHISPER acoustic tracking system [15]. Vallidis uses a spread spectrum acoustic solution to compensate for blocking by the body. The signals must then be filtered to determine

the distance between the sensors. In contrast to our work, this work is limited to a specific type of motion tracking and we address blocking with placement and numbers of sensors.

Another notable motion tracking system outside of acoustic and camera tracking is Measurand's ShapeTape [16], based on fiber optics. This device tracks the bending and twisting of the tape with respect to the placement on the body in 3D.

III. DESIGN ISSUES

This section describes the theory of operation of the proposed system, the sources of error in the measurements, and potential physical media for implementing it.

A. Theory of Operation

The technique we employ for finding the location of a point on the body is a form of triangulation called *lateration*, which uses distances from several known reference points, illustrated in Figure 1. This is the same basic technique that is employed by the Global Positioning System (GPS) to find locations of points on the surface of the Earth [17]. For our application, we place the reference points on the torso and assume that the positions of those reference points are relatively stable. Section V explores the validity of this assumption.

Ideally, in three-dimensional space a minimum of four reference points is required to locate a point using lateration. In practice, however, because of errors in the distance measurements, using more than the minimum number of reference points can increase the accuracy of the location estimate. The simulation results presented in Section V show that using more than four reference points increases the accuracy for this application. We plan to place emitters at the reference points and receivers on the limbs; they will be connected with a synchronization signal through the e-textile. The system could also work with receivers on the reference points and emitters on the limbs. However, for the first order study we are describing here, whether the reference points are emitters or receivers does not matter.

B. Sources of Error

There are several sources of error that we consider in the simulation of our application of lateration. The first stems from our assumption that the reference points on the torso are fixed relative to each other. In reality, they are not fixed, and the change in distance between them will introduce errors into the location estimation. The torso is not a static plane but a dynamic interaction of the shoulders rotating with respect to the waist to maintain a person's balance for various motions. To better illustrate this, consider a user walking: the arms swing in line, with the hips rotating as the legs move, producing a small sway of the hips and shoulders. With running, however, the arms pump as the legs bend and step forward; with each pump of the arm the shoulders move much larger distances relative to the hips and sternum than they do during walking. This motion of the torso introduces an inherent error in the lateration calculation. Even with a perfectly form

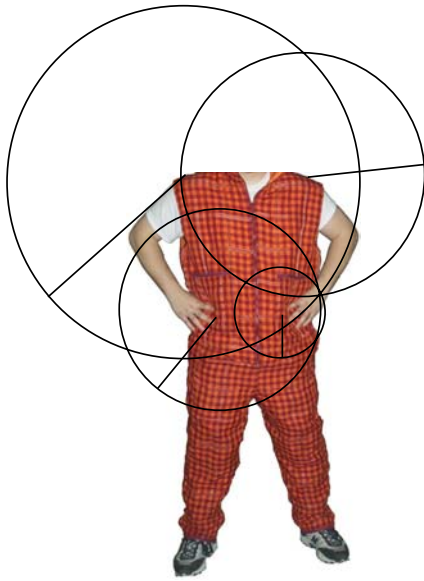


Fig. 1. An illustration of lateration using four reference points (two on the shoulders and two on the waist). The spheres from these four points intersect at a point on the user's left wrist.

fitting garment there will be an intrinsic amount of error due to torso movement.

The second source of error is due to shadowing, the user's body or clothing blocking the signal used to calculate time of flight. If the physical media requires line of sight in order to function, then when the line of sight is blocked between one or more of the reference points and the point on the limb, the location estimate may not be possible. This is one of the reasons Section V examines the effect of using more than the minimum number of reference points.

The third source of error stems from the directivity of the emitters. Most emitters do not transmit the signal at equal strength in all directions. In some directions, little or no signal may be transmitted. Consequently, even when there is a line of sight between a reference point and the point on the limb, if the emitter is facing in the wrong direction, then the distance for that pair cannot be determined. Receivers may also have a directivity, so the same argument can be applied to them.

There are other sources of errors that we do not consider in our simulation, for example, the resolution of the time-of-flight measurement and multipath signals when a line-of-sight does not exist. However, we believe these are second-order effects compared to the three sources above.

C. Physical Media

There are several physical media that can be used to determine distance via time-of-flight. Our initial plan is to use ultrasound, due to its ease of implementation, low cost, and low power. We have made some initial observations of the blocking effects of the body and cloth on ultrasound using Ultrasound Design Kit (part number 0-1005870-1) from Measurement Specialties, Inc. [18]. Based on our observations, the body will block the signals, and cloth will greatly attenuate it. For example, the signal is still apparent when passing through one layer of denim, but two layers will essentially

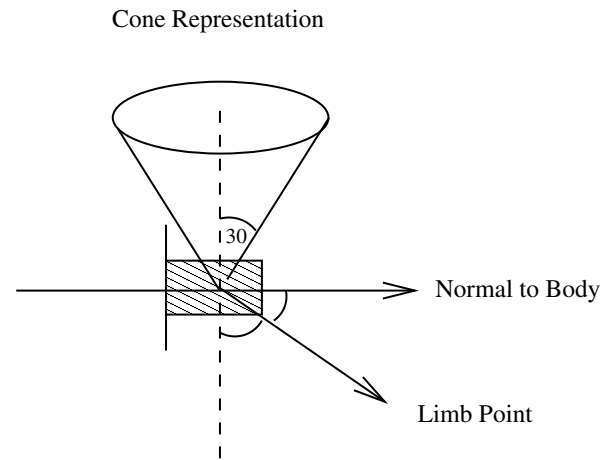


Fig. 2. Illustration of directionality of the ultrasonic emitters. The cone is the cross section of the beam. The full beam is the volume swept when the cone is rotated 360° around the line labeled "Normal to body".

block it. The emitters have a wide beam directivity that is suited to this application, as illustrated by Figure 2. The axis of the emitter is the line labeled "normal to body" in the figure; the cross section of the beam emitted is a cone with an axis perpendicular to the axis of the emitter. Thus the full beam of the emitter is the volume swept by cone in the figure when it is rotated 360° around the axis of the emitter. The angle of the cone measured from its axis is 30° . When mounted on the body, the beam from these emitters will tend to be aimed along the body rather than away from it. In the results presented in Section V, a point on the limb is considered to be in the beam if the line segment between the point and the center of the emitter falls within the cone's 30° angle from its axis.

An interesting alternative for measuring distance is ultra-wideband (UWB) radio. Due to the resolution of the pulses required for UWB transmission, it is possible to use time-of-flight between a transmitter and receiver to measure distances with an error of less than 1 cm [19]. At the current time, UWB devices are expensive and not readily available. Furthermore, we are not aware of any time-of-flight experiments conducted through or near the human body, so we are not sure if shadowing by the body will be an issue. Finally, the power consumption of UWB receivers may be larger than for ultrasound because of the digital signal processing requirements.

IV. SIMULATION METHOD

To model the system, we created a simulation that was driven by motion capture data from Carnegie Mellon University [20]. The location of the markers in the capture data and their abbreviations are shown in Figure 3. Thirty eight files of capture data were used for the simulations; these files contained sixteen subjects and six motions (walk, run, jump, dance, swordplay, and basketball). Not all motions were available for each subject.

A non-linear least squares fit was used to estimate the location of a point on a limb. For each reference point i on the torso, using the equation

$$f_i = R_i^2 - ((x_i - x)^2) + (y_i - y)^2 + (z_i - z)^2 \quad (1)$$

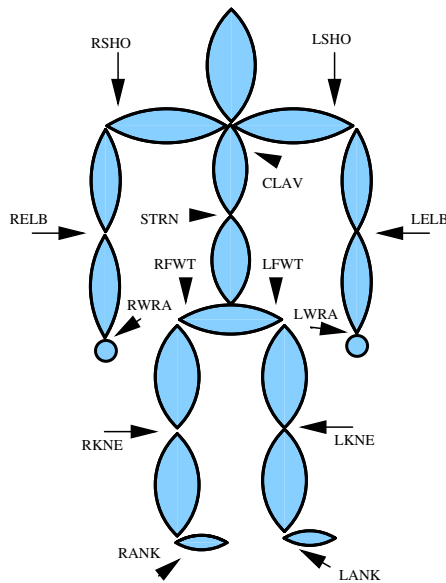


Fig. 3. An illustration of the location of the markers in the motion capture data. Three markers on the back (upper back, back left waist, back right waist) are not shown.

$\|f\|$ was minimized with Matlab's non-linear least squares solver, where f is a vector-valued function with the i^{th} component of f equal to f_i , R_i is the distance from the reference point i to the limb point, x_i, y_i , and z_i are the coordinates of the reference point, and x, y , and z are the coordinates of the limb point that are being solved for. For four reference points, there is an exact solution such that $\|f\| = 0$. When there are more than four reference points, the system is overdetermined and $\|f\|$ will likely be non-zero.

Simulation allows us to study the sources of error described in Section III across a broad segment of the population and motions before building a first prototype. Our goal for simulation is to reduce the number of iterations of prototypes that must be built by removing the some of the inherent difficulties involved with human subjects. Having a test subject wearing a prototype exactly reproduce a motion repeatedly is impossible, so that it is difficult to experimentally isolate the effect of a change in the prototype. Using simulation based on motion capture data, the exact motion is always reproducible by simply using the same motion data repeatedly. However, there are other sources of error, such as reflections from the environment, that we do not consider in our simulations. These sources will be evaluated with our first prototype, and incorporated into future simulations as necessary.

V. RESULTS

Our simulations covered three major sources of error in the lateration calculation: Movement of the reference points on the torso, shadowing of the physical signals by the body, and directivity of the transmission of the physical signals.

The first set of simulations examined the stability of the points on the torso. Table I shows the standard deviation of the distance from each point on the torso to every other point on the torso for the walking and running motions (11 subjects), while Table II shows the standard deviation of

the distances between torso points for all motions (running, walking, jumping, dancing, swordplay, and basketball; 16 subjects). For walking and running, the largest deviations are in the range of 10 mm. As expected, for all the motions the deviations are larger, but even so the largest value (lsho-rsho) is only 18 mm. Space does not permit showing the data for each individual motion and user, but in looking at individual motions with large deviations we have noticed that while one or two torso points may have larger than usual values most of the other points usually do not. For example, the motion that had the largest standard deviation was playing basketball; examination of the video shows that the subject was dribbling the basketball in his right hand while walking backwards. The right shoulder had very large movements relative to the other torso points, but the other points were essentially fixed. Based upon these results, we believe the points on the torso are relatively stable with respect to each other, even over a wide range of motions including those that are more animated (e.g., dancing, swordplay) than may be expected from a user going about a normal daily routine.¹

TABLE I

STANDARD DEVIATION OF DISTANCES BETWEEN ALL TORSO POINTS FOR WALKING AND RUNNING MOTIONS, MM

	rsho	lsho	clav	strn	rfwt	lfwt	rbwt	lbwt
lsho	3.14							
clav	2.90	2.38						
strn	2.81	2.43	1.51					
rfwt	8.93	6.60	9.61	10.42				
lfwt	6.54	7.97	9.03	10.01	1.69			
rbwt	7.53	9.26	6.23	5.39	3.94	4.33		
lbwt	9.45	6.98	6.11	5.27	4.04	3.93	0.88	
ubac	3.36	3.14	4.73	3.76	4.28	4.15	6.11	5.65

TABLE II

STANDARD DEVIATION OF DISTANCES BETWEEN ALL TORSO POINTS FOR ALL MOTIONS (WALKING, JUMPING, RUNNING, DANCING, SWORDPLAY AND BASKETBALL), MM

	rsho	lsho	clav	strn	rfwt	lfwt	rbwt	lbwt
lsho	17.81							
clav	5.09	4.82						
strn	5.09	4.74	3.43					
rfwt	15.89	9.72	12.06	11.69				
lfwt	8.79	15.21	10.77	11.06	2.30			
rbwt	13.20	13.26	9.71	8.36	3.69	3.68		
lbwt	13.00	14.09	9.70	8.49	3.95	3.15	1.45	
ubac	6.84	6.98	5.29	4.34	6.84	7.07	10.56	10.74

Another question we studied was whether the movement of the torso points depends upon body size. Figure 4 shows the standard deviation of the distance from the sternum to clavicle, sternum to right waist, and sternum to right shoulder as a function of the knee to ankle length of the subject. The points for the left side of the body are omitted for clarity; they are similar in shape and value to those for the right side. To isolate the effect of body size, we looked at data sets for users making the same motions. The results shown are for walking,

¹We expect these motions are somewhat out of the ordinary except for users who earn their living making them, such as dancers and Jedi knights.

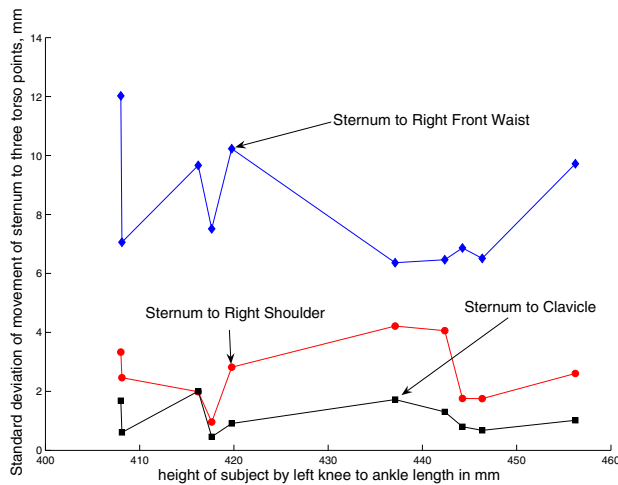


Fig. 4. Standard deviation of the distances between several points on the torso versus body size for sternum to clavicle, right waist, and right shoulder. Left waist and shoulder are omitted for clarity; their distances are similar to right waist and shoulder.

a total of ten subjects. No clear correlation is visible, so we believe that the stability of the torso reference points is not a function of the user's body size.

Given that the torso points were relatively stable across a range of motions and body sizes, the remaining simulations examined the accuracy of locating points on the limbs. These calculations were made for the ankles (RANK and LANK markers in Figure 3), knees (RKNE, LKNE), wrists (RWRA, LWRA), and elbows (RELB, LELB). The actual distance between the point on the limb and each of the reference points was calculated. But in making the lateration calculations it was assumed the reference points were a fixed distance apart, i.e., the actual positions of the reference points were not used. This gives rise to the first source of error described in Section III.

We did not exhaustively test every possible combination of four to nine sensors for the reference points. Instead we used an iterative, heuristic process of removing the reference point that at each step had the least effect on the error. We calculated the average and maximum error for each limb point using all nine reference points and then for each combination of eight reference points. We then looked for the set of eight reference points whose maximum error was closest to that for using all nine reference points. The reference point that did not belong to this set of eight had the least impact on the accuracy of the system and so could be removed. We repeated this process for each number of reference points, e.g., with eight reference points, we calculated the average and maximum error for all combinations of seven reference points and then chose the set of seven whose results were most nearly as good as using eight reference points. We used the maximum error as our metric for comparing the quality of the solutions, but a case could be made for using other metrics to eliminate reference points, such as the average error over all of the limb points. Space does not permit showing the results from all of the combinations that we simulated (40), so we have chosen combinations with the best and the worst

maximum error for each number of reference points to give an indication of the change in quality and range of results as the number of reference points is reduced. For all of the data presented in the remainder of the paper, we will consistently use the same pairs of configurations that we chose based upon the best and worst maximum error considering only torso movement for the jumping, basketball, dancing, and swordplay motions, and present them in the same order. For the results presented in the remainder of the paper we use the labels for the configurations shown in Table III.

TABLE III
LABELS FOR CONFIGURATIONS OF REFERENCE POINTS

Configuration	Label
rsho lsho rfwt lfwt strn clav ubac rbwt lbwt	9
rsho lsho rfwt lfwt clav ubac rbwt lbwt	8A
rsho lsho rfwt strn clav ubac rbwt lbwt	8B
rsho lsho rfwt lfwt ubac rbwt lbwt	7A
rsho lsho rfwt clav ubac rbwt lbwt	7B
rsho lsho rfwt lfwt ubac rbwt	6A
rsho lsho lfwt ubac rbwt lbwt	6B
rsho lsho rfwt lfwt ubac	5A
rsho lsho rfwt ubac rbwt	5B
rsho lsho rfwt lfwt	4A
lsho rfwt lfwt ubac	4B

Table IV and Table V show the average and maximum error for locating the points of the limb when only the movement of the reference points is taken into account, without considering blocking by the body or directivity. Table IV shows the error for the walking and running motion, while Table V shows the error for all the other motions (jumping, basketball, dancing, and swordplay).

As expected, the average and maximum errors are much larger for the more animated motions than for walking and running. The data also shows the benefit of using more than the minimum number of reference points. While the average error for walking and running is about the same for four reference points and nine reference points, using nine reference points has a much lower maximum error. Furthermore, for the other motions, both the average error and the maximum error are much worse for four reference points than they are for nine. But from six to eight reference points, the average and maximum are only slightly worse than for nine.

Tables VI and VII show the effect of body shadowing and directivity for all motions versus the reference points that are used. To approximate the user's body for the shadowing, the points from the motion data were fitted to a set of cylinders to represent the limbs and torso [21], as illustrated in Figure 5. The cylinder representation of the body model is a first order approximation that allowed us to start simulation without the cost associated with an absolute body model. This method does not allow us to consider various body types or weights, however, it did give us an opportunity to determine if this is a viable method for motion tracking.

The body was considered to block the transmission if the line segment from the reference point on the torso to the point on the limb intersected a cylinder. For the effect of the directivity of the transmitters, our initial candidate for the physical medium was ultrasound. As described in Section III

TABLE IV
AVERAGE AND MAXIMUM ERROR OF LOCATION ESTIMATE OF LIMB POINTS FOR WALKING AND RUNNING, MM

Reference Points	ankles		knees		wrists		elbows	
	avg	max	avg	max	avg	max	avg	max
9	16.24	50.51	8.21	29.95	3.88	46.27	3.47	34.79
8A	16.72	51.67	8.46	29.99	4.08	46.07	3.79	34.70
8B	11.46	46.42	6.64	28.30	4.11	56.26	3.41	36.36
7A	17.12	51.79	8.68	30.53	4.31	45.47	3.89	34.39
7B	12.48	55.09	7.00	29.82	4.47	56.49	3.97	35.96
6A	17.72	53.83	9.21	41.91	4.51	45.98	3.86	34.55
6B	13.50	66.62	7.48	32.59	4.45	44.97	3.86	34.40
5A	18.77	101.78	10.49	93.73	5.07	68.71	3.98	26.63
5B	14.18	59.93	8.00	41.21	4.93	56.38	4.15	35.94
4A	39.46	347.12	31.40	228.49	18.42	134.67	7.53	125.33
4B	31.21	116.26	17.68	103.84	7.79	75.42	5.26	55.23

TABLE V
AVERAGE AND MAXIMUM ERROR OF LOCATION ESTIMATE OF LIMB POINTS FOR ALL OTHER MOTIONS (JUMPING, DANCING, SWORDPLAY AND BASKETBALL), MM

Reference Points	ankles		knees		wrists		elbows	
	avg	max	avg	max	avg	max	avg	max
9	24.85	126.20	14.70	80.77	13.33	125.94	10.65	112.97
8A	26.12	127.32	15.38	80.90	14.04	125.72	11.22	113.00
8B	29.49	169.16	18.42	106.34	14.33	91.78	11.61	72.41
7A	27.02	127.79	15.94	85.90	15.00	127.58	11.71	116.95
7B	30.66	168.33	19.12	111.84	15.51	91.95	12.63	77.02
6A	28.46	131.74	17.13	87.66	14.75	121.58	10.96	110.34
6B	32.07	188.00	20.17	147.33	15.05	128.62	12.52	116.80
5A	32.75	139.14	19.93	91.44	15.39	99.35	10.40	87.31
5B	33.95	212.71	21.77	150.04	17.01	94.00	12.68	80.52
4A	96.58	534.37	67.54	347.17	41.57	282.94	25.79	313.00
4B	39.77	176.68	23.01	102.15	21.58	205.42	13.70	142.37

and illustrated in Figure 2, the beam for our ultrasonic emitter has a wide directivity that will tend to be aimed along the body. For these results, a point on the limb was considered to be in the beam from the emitter if the line segment between the point and the center of the emitter is within the cone's 30° angle from its axis and is shadowed by the body.

The body shadowing and directivity data was calculated over all motions for ankles, knees, wrists, and elbows; left and right were considered together for these calculations. The "body" columns of the table are for blocking only. The values in the "body" columns are the percentage of time that a point on a limb has a line of sight to less than four reference points, and thus it will not be possible to perform the lateration calculation; smaller numbers are better. The "unavail" columns take into account both blocking and directivity; these columns show the percentage of time that a point on the limb was visible to less than four reference points due to either body blocking or being out of the beam. As the data in the table shows, as the number of reference points is reduced, the inability to make a location estimate for the limb points increases very quickly. With nine reference points, the unavailability of the wrists is 33%, while for six reference points, the unavailability is 51%, and for four reference points, it jumps to over 80%.

An important point to take from this table is that blocking by the body has less of an impact than directivity. The ankles and the wrists are blocked a small percentage of the time, but knees and elbows almost never are. However, the availability of the elbows and especially the wrists is low, much lower than for the ankles and knees. The reason for this is that the region covered by the beam gets larger as the distance from the torso increases. The elbows and wrists are usually much closer to the torso where the range covered by the beam is much smaller than it is for the more distant knees and ankles.

Finally, the right half of Table VI and Table VII shows the average and maximum error when both blocking and directivity are taken into account for walking/running and all other motions, respectively. The data in this table is the error when at least four reference points are visible; when less than four points are visible, no location estimate was made². For example, the average and maximum errors for six sensors is better than that for nine sensors; however, the unavailability for six sensors is much worse than for nine. To allow for comparison with Tables IV and V, the same combinations of reference points are shown in all four tables. As expected, the

²We chose not to artificially increase the error when a point was unavailable. Thus one must take availability and error into account.

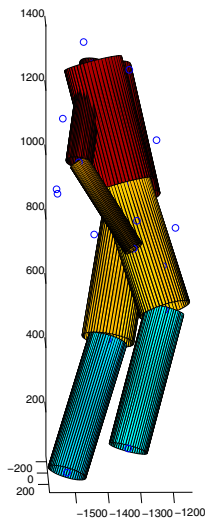


Fig. 5. Cylinders fit to the motion capture markers as a model for the body for use in body shadowing simulations. Units for the X,Y, and Z axes are cm.

errors when blocking and directivity are taken into account are generally worse than when they are not taken into account. The average errors are only slightly worse, but the maximum errors are much larger.

VI. CONCLUSIONS AND FUTURE WORK

This paper has explored the feasibility of constructing a wearable, self-contained full-body motion capture system based on time-of-flight measurements. We believe that the system is feasible for many applications. The size of the errors based solely upon the movement of the reference points will make this system less accurate than state-of-the-art laboratory-based motion capture systems, which have accuracies of a few millimeters. The system is potentially accurate enough to be used for context-awareness, user interfaces, and in-the-field biomechanical studies. The directivity of the physical media chosen for the time-of-flight measurements is the main factor in the accuracy of the system.

There are several avenues that we would like to pursue for future work. One area is to look for ways to improve the accuracy of the system, particularly the maximum errors. We intend to examine the effect of using both rate-of-change and time-of-flight sensors. As Welch noted in [22], a combination of rate-of-change and absolute distance sensors will likely provide a better solution than either alone. The absolute distance sensors can periodically provide boundary conditions and error corrections to the rate-of-change sensors. Another modification that we intend to examine is to incorporate a model of the body such as the fourteen-segment body model in [23] into the non-linear least squares fit. Such a model would provide an additional constraint on the solution besides the time-of-flight information. For example, a body model might allow us to make an estimate of where a limb is when it is shadowed by the body. We will expand our current simulation to include both of these methods, and then we intend to build a physical prototype of the system.

Once the prototype has been implemented, we plan to develop the software location services based on shape-sensing. The first services that we will likely implement are for finding spacing of sensors, e.g. for acoustic beamforming, and for having sensing and processing nodes automatically determine their location on the body. In our current prototypes, each node must be hard coded with its location on the garment, and if it is detached from the garment, it must be returned to the same location or else the application will fail. It is desirable to have a node automatically sense its location on the body so that an application writer can program the garment as a whole rather than as a collection of individual nodes.

We would also like to explore context-awareness algorithms that are based on the shape of the body. Most wearable context-awareness applications for determining user activity are based on derivatives of activity, e.g. [24] and [25]. We suspect that having the absolute shape of the body will open up other methods of classification that are more similar to those used in image processing and feature recognition.

As a closing note, we believe that the design approach we have taken here, using simulation for initial exploration of the design space before jumping into building a prototype and improving it through trial-and-error, is one that should be encouraged in the wearable computing community. This method allowed us to more easily determine data across population types without the time and resource constraints of building prototypes for a broad range of users. For example, studying the effect of height on movement of the torso points would have been very time and labour intensive using only prototypes. While simulation may not be appropriate for every design situation, the wearable computing field is mature enough that it is becoming increasingly viable.

ACKNOWLEDGMENT

This material is based upon work supported by the National Science Foundation under Grant No. CCR-0219809 and CNS-0447741.

REFERENCES

- [1] M. Jones, T. Martin, and Z. Nakad, "A service backplane for e-textile applications," in *Workshop on Modeling, Analysis, and Middleware Support for Electronic Textiles*. MAMSET 2002, October 2002, pp. 15–22.
- [2] T. Martin, M. Jones, J. Edmison, and R. Shenoy, "Towards a design framework for wearable electronic textiles," in *Proceedings of the Seventh International Symposium on Wearable Computing*. ISWC 2003, October 2003, pp. 190–199.
- [3] D. Marculescu, R. Marculescu, N. Zamora, P. Stanley-Marbell, P. Khosla, S. Park, S. Jayaraman, S. Jung, C. Lauterbach, W. Weber, T. Kirstein, D. Cottet, J. Grzyb, G. Troester, M. Jones, T. Martin, and Z. Nakad, "Electronic textiles: A platform for pervasive computing," *Proceedings of the IEEE*, vol. 91, pp. 1995–2018, 2003.
- [4] E. Post, M. Orth, P. Russo, and N. Gershenfeld, "E-broidery design and fabrication of textile-based computing," *IBM Systems Journal*, vol. 39, no. 3 and 4, 2000.
- [5] S. Park, C. Gopalsamy, R. Rajamanickam, and S. Jayaraman, "The wearable motherboard: An information infrastructure or sensate liner for medical applications," *Studies in Health Technology and Informatics, IOS Press*, vol. 62, pp. 252–258, 1999.
- [6] T. Kirstein, D. Cottet, J. Grzyb, and G. Troester, "Textiles for signal transmission in wearables," in *Workshop on Modeling, Analysis, and Middleware Support for Electronic Textiles*. MAMSET 2002, October 2002, pp. 9–14.

TABLE VI

EFFECT OF BODY SHADOWING AND DIRECTIVITY %, AVERAGE AND MAXIMUM ERROR OF LOCATION ESTIMATE OF LIMB POINTS FOR WALKING AND RUNNING WITH BLOCKING AND BEAM DIRECTIVITY INCLUDED, MM,

Reference Points	ankles		knees		wrists		elbows		ankles		knees		wrists		elbows	
	body	unavail	body	unavail	body	unavail	body	unavail	avg	max	avg	max	avg	max	avg	max
9	0.00	0.27	0.00	0.98	1.79	27.55	0.00	2.33	18.44	90.81	10.05	160.82	7.79	155.13	4.68	46.68
8A	0.00	0.27	0.00	0.98	1.79	30.14	0.00	2.59	18.44	90.81	10.05	160.82	7.84	155.13	4.77	46.68
8B	1.16	1.70	0.00	2.33	2.15	33.01	0.00	2.77	14.75	107.66	8.36	87.29	6.16	62.14	4.17	35.96
7A	0.00	0.89	0.00	1.16	1.97	45.80	0.00	3.13	20.83	347.12	12.05	228.49	8.36	104.43	6.53	125.33
7B	1.16	1.70	0.00	2.33	2.15	35.96	0.00	3.04	14.75	107.66	8.36	87.29	6.19	59.89	4.24	35.96
6A	0.89	8.59	0.00	1.16	2.33	47.14	0.00	10.73	21.68	347.12	12.44	228.49	8.55	104.43	6.77	125.33
6B	1.79	4.03	0.00	5.72	2.50	56.80	0.00	8.68	17.38	302.87	7.97	93.17	4.12	60.52	3.91	37.89
5A	4.74	31.48	0.00	3.40	2.33	52.86	0.00	18.69	25.67	347.12	13.26	228.49	9.98	112.73	6.67	125.33
5B	4.74	14.13	0.00	5.72	2.50	59.12	0.00	21.56	18.35	120.92	8.36	87.76	4.52	59.11	4.22	35.94
4A	37.03	69.86	0.45	7.07	4.20	63.68	0.00	50.00	28.93	347.12	32.28	228.49	23.68	134.67	9.35	125.33
4B	19.77	53.31	0.63	11.36	3.40	74.42	0.00	59.30	28.06	102.14	16.95	103.84	4.76	60.30	4.73	55.23

TABLE VII

EFFECT OF BODY SHADOWING AND DIRECTIVITY %, AVERAGE AND MAXIMUM ERROR OF LOCATION ESTIMATE OF LIMB POINTS FOR ALL OTHER MOTIONS, WITH BLOCKING AND BEAM DIRECTIVITY INCLUDED, MM

Reference Points	ankles		knees		wrists		elbows		ankles		knees		wrists		elbows	
	body	unavail	body	unavail	body	unavail	body	unavail	avg	max	avg	max	avg	max	avg	max
9	0.26	2.56	0.00	6.45	0.51	35.60	0.00	13.92	30.49	230.60	18.81	225.63	21.20	217.01	13.04	187.15
8A	0.26	2.56	0.00	7.18	0.51	37.51	0.00	15.71	30.81	230.60	19.01	225.63	20.71	154.86	12.14	142.69
8B	1.03	5.28	0.00	8.64	0.59	40.40	0.00	16.19	35.88	244.63	21.30	225.63	22.88	217.01	14.22	187.15
7A	0.26	3.15	0.00	9.05	0.84	47.84	0.00	18.35	33.24	248.07	19.24	206.94	20.87	154.86	12.55	156.61
7B	1.10	5.31	0.00	9.30	0.59	42.42	0.00	18.17	36.08	231.85	21.57	225.63	22.48	112.41	13.27	140.14
6A	1.28	7.33	0.22	9.27	1.03	52.60	0.00	20.18	33.72	291.44	20.57	206.94	19.80	154.86	11.78	156.61
6B	1.32	7.25	0.22	14.10	1.06	58.35	0.37	22.71	39.26	321.85	21.15	131.04	17.45	122.88	12.46	126.11
5A	5.49	16.92	0.70	12.05	1.76	60.55	0.04	25.79	36.85	248.07	22.44	206.94	17.97	154.86	11.52	202.16
5B	5.53	14.65	0.70	14.76	2.05	65.86	0.11	27.03	42.53	349.79	22.69	150.04	17.30	137.50	12.09	73.83
4A	25.79	42.12	2.31	16.41	6.92	70.04	1.21	51.17	96.15	534.37	72.02	336.88	60.13	282.94	28.35	313.00
4B	17.58	35.20	2.42	20.70	7.33	74.94	1.14	52.27	38.16	151.96	22.23	91.51	14.03	103.87	10.44	78.19

- [7] F.-C. Chan, F. Dabiri, R. Jafari, E. Kursun, V. Raghunathan, T. Schoellhammer, D. Sievers, D. Estrin, G. Reinman, M. Sarrafzadeh, M. Srivastava, B. Wu, and Y. Yang, "Reconfigurable fabric: An enabling technology for pervasive medical monitoring," in *Proceedings of Communication Networks and Distributed Systems: Modeling and Simulation*, January 2004.
- [8] Eleksen, Ltd., 2004. [Online]. Available: <http://www.eleksen.com>
- [9] S. Jung, C. Lauterbach, and W. Weber, "Integrated microelectronics for smart textiles," in *Workshop on Modeling, Analysis, and Middleware Support for Electronic Textiles*. MAMSET 2002, October 2002, pp. 3-8.
- [10] S. Basu, S. Schwartz, and A. Pentland, "Wearable phased arrays for sound localization and enhancement," in *Proceedings of the Fourth IEEE International Symposium on Wearable Computers*. ISWC 2000, 2000, pp. 103-110.
- [11] J. Edmison, M. Jones, Z. Nakad, and T. Martin, "Using piezoelectric materials for wearable electronic textiles," in *Proceedings of the Sixth International Symposium on Wearable Computing*. ISWC 2002, 2002, pp. 41-48.
- [12] D. Sutherland, "The evolution of clinical gait analysis: Part ii," *Kinematics, Gait and Posture*, vol. 16, no. 2, pp. 159-179, 2002.
- [13] E. Foxlin and M. Harrington, "Weartrack: A self-referenced head and hand tracker for wearable computers and portable vr." in *4th International Symposium on Wearable Computers*, October 2000, pp. 155-162.
- [14] —, "Miniature 6-dof inertial system for tracking hmds," in *SPIE Conference on Helmet- and Head-Mounted Displays*, April 1998.
- [15] N. M. Vallidis, "Whisper: A spread spectrum approach to occlusion in acoustic tracking," Ph.D. dissertation, Department of Computer Science, The University of North Carolina at Chapel Hill, 2002.
- [16] "Shapetape." [Online]. Available: <http://www.measurand.com/products/ShapeTape.html>
- [17] J. Hightower and G. Borriello, "Location systems for ubiquitous computing," *IEEE Computer*, vol. 34, no. 8, pp. 57-66, August 2001.
- [18] Measurement Specialties Inc., "Piezo film sensors product guide and price list," 2004. [Online]. Available: http://www.msusa.com/download/pdf/english/piezo/catalog_price_list.pdf
- [19] J. Adams, W. Gregorwich, L. Capots, and D. Liccardo, "Ultra-wideband for navigation and communications," in *Proceedings of the IEEE Aerospace Conference*, march 2001, pp. 785-792.
- [20] CMU Graphics Laboratory, "CMU Graphics Lab Motion Capture Database," 2003. [Online]. Available: <http://mocap.cs.cmu.edu/search.html>
- [21] M. Black, "3d body model," 2004. [Online]. Available: <http://www.cs.brown.edu/courses/cs296-4/homework2.htm>
- [22] G. Welch and E. Foxlin, "Motion tracking: No silver bullet, but a respectable arsenal," *IEEE Computer Graphics and Applications*, vol. 22, no. 6, pp. 24-38, 2002.
- [23] T. Lockhart, J. Woldstad, and J. Smith, "Effects of age-related gait changes on biomechanics of slips and falls," *Ergonomics*, vol. 46, no. 12, pp. 1136-1160, 2003.
- [24] K. Van Laerhoven, A. Schmidt, and H. Gellerson, "Multi-sensor Context Aware Clothing," in *Proceedings of the Sixth International Symposium on Wearable Computers*, 2002, pp. 49-57.
- [25] A. Golding and N. Lesh, "Indoor Navigation Using a Diverse Set of Cheap Wearable Sensors," in *Proceedings of the Third International Symposium on Wearable Computers*, 1999, pp. 29-36.